# Raman Scattering Reveals Ion-Dependent G-Quadruplex Formation in the 15-mer Thrombin-Binding Aptamer upon Association with Alpha-Thrombin

Grant J. Myres, Jay P. Kitt, and Joel M. Harris\*

Department of Chemistry, University of Utah, 315 South 1400 East

Salt Lake City, UT 84112-0850 USA

#### **Abstract**

Discovery of DNA aptamers that bind biomolecular targets has enabled significant innovations in biosensing. Aptamers form secondary structures that exhibit selective, high-affinity interactions with their binding partners. Binding of its target by an aptamer is often accompanied with conformational changes, where sensing by aptamers often relies on these changes to provide readout signals from extrinsic labels to detect target association. Many biosensing applications involve aptamers immobilized to surfaces, but methods to characterize conformations of immobilized aptamers and their in-situ response have been lacking. To address this challenge, we have developed a structurally informative, Raman spectroscopy method to determine conformations of the 15-mer thrombin-binding aptamer (TBA) immobilized on porous silica surfaces. TBA is of interest because its binding of alpha-thrombin depends on the aptamer forming an anti-parallel G-quadruplex, which is thought to drive signal changes that allow thrombinbinding to be detected. However, specific metal cations also stabilize the G-quadruplex conformation of the aptamer even in the absence of its protein target. To develop deeper understanding of the conformational response of TBA, we utilize Raman spectroscopy to quantify the effects of the metal cations, K<sup>+</sup> (stabilizing) and Li<sup>+</sup> (non-stabilizing), on G-quadruplex versus unfolded populations of TBA. In K<sup>+</sup> or Li<sup>+</sup> solutions, we then detect association of alpha-thrombin with the immobilized aptamer, which can be observed in Raman scattering from the bound protein. The results show that association of alpha-thrombin in K<sup>+</sup> solutions produces no detectable change in aptamer conformation, which is found in G-quadruplex form both before and after binding its target. In Li<sup>+</sup> solutions, however, where TBA is unfolded prior to alpha-thrombin association, protein binding occurs with formation of a G-quadruplex by the aptamer.

\* Corresponding author: harrisj@chem.utah.edu

#### INTRODUCTION

In addition to being the biopolymer that encodes genetic information, DNA has also had significant impacts in biotechnology.<sup>1-6</sup> One innovation is the discovery and applications of aptamers;<sup>7-9</sup> DNA aptamers are short sequences of non-genomic, single-stranded DNA that, like antibodies, selectively bind a range of target molecules including proteins,<sup>10</sup> carbohydrates,<sup>9,11</sup> and small molecules.<sup>12-14</sup> Because of their broad range of molecular targets, stability, and ease of synthesis and amplification,<sup>15</sup> DNA aptamers offer opportunities and distinct advantages<sup>1,16</sup> over antibodies in certain biosensing applications.

Critical in development and application of DNA aptamers in biosensing is to understand the relationship between aptamer secondary structure and its binding of a target molecule. 17-20 Although some aptamers have been shown to adopt an association-state conformation prior to binding, 21,22 other aptamers undergo conformation changes in response to interactions formed with a target molecule. 23,24 A major development in aptamer-based sensing technologies has been to harness conformational changes as a means of detecting aptamer-bound analytes. 25-28 By modifying aptamers with either redox probes 25,28 or combinations of fluorophores and quenchers, 21,27 a measurable signal change (current or fluorescence, respectively) can be detected in response to analyte binding. The measured responses of these aptamers, however, provide only indirect evidence of a change in conformation upon target binding and are not directly informative of structure.

The aptamer response, in addition to being sensitive to primary sequence, can be confounded by interactions with off-target molecules<sup>14,29</sup> and by conformational changes that are sensitive to ionic strength<sup>21</sup> or the presence of specific ions in solution.<sup>30</sup> Experimental approaches to investigate the molecular basis for a target-binding response should thus provide insight into the many factors that govern the aptamer conformation. Spectroscopic methods such as circular dichroism (CD)<sup>19,23,24,31</sup> and NMR<sup>29,32,33</sup> have been used to investigate aptamer structures in free-solution. These methods can reveal structural information and conformational changes, but neither method is suitable for investigating surface-immobilized aptamers. Recent advances in aptamer-based biosensing are based on DNA tethered to solid supports, allowing a response to targets that bind from solution.<sup>34,35</sup> Unfortunately, information acquired about aptamer structure in free solution may not apply to aptamers immobilized on solid surfaces, whose structure and target

binding can differ from free solution due to surface-immobilization,<sup>19</sup> interfacial electrostatics,<sup>36</sup> entropic effects,<sup>37</sup> and local crowding,<sup>38</sup> interactions that are not present in free-solution.<sup>19</sup>

Despite the need for quantitative, structurally informative methods to investigate immobilized aptamers and their binding response at interfaces, few surface-sensitive techniques can provide the structural insights to characterize these interactions. Infrared-reflection<sup>39-41</sup> and sum-frequency generation<sup>42-45</sup> spectroscopies have been previously applied to characterize immobilized DNA, but these methods have not been used to quantify conformational changes when targets bind to immobilized aptamers. Although Raman spectroscopy has been applied to investigate the structure of DNA in free-solution, 46-50 its application to investigating DNA aptamers immobilized at surfaces is challenged by the fact that Raman scattering cross sections are small ( $\sigma \approx 10^{-28}$  cm<sup>2</sup>). This sensitivity challenge can be overcome by enhancement of scattering cross sections at plasmonic substrates, which has allowed surface-enhanced Raman spectroscopy (SERS) to detect DNA aptamers and binding of protein targets at coinage-metal surfaces. 51-54 Despite the success of SERS in detecting surface-bound aptamers, there are significant challenges with employing this method to investigate aptamer structure at interfaces. The quantitative response and reproducibility of SERS spectra of DNA can vary with differences in orientation<sup>55,56</sup> and distance from the plasmonic-metal surface, <sup>57,58</sup> factors that can depend on surface-density of bound aptamers, leading to irreproducibility in response upon binding of a target protein.<sup>51</sup>

Recently, we have reported an alternative means of overcoming sensitivity limitations of Raman scattering by immobilizing DNA onto the interior surfaces of porous silica particles and detecting the internal composition of these particles with confocal-Raman microscopy. Due to the high specific surface areas of these materials, densities of DNA immobilized on their internal surfaces can produce within-particle DNA concentrations as high as ~30 mM,<sup>59</sup> exceeding concentrations required for Raman scattering detection. Because silica is a purely dielectric material and the internal surfaces of the porous material are randomly oriented, Raman scattering is independent of both orientation and proximity of the oligonucleotide relative to the silica surface. This attribute allows the Raman scattering intensities to report the surface-density of immobilized DNA,<sup>59</sup> to determine hybridization efficiency of fully- and partially-complementary DNA,<sup>60</sup> and to quantify molecules from nanomolar solutions that bind to immobilized DNA strands.<sup>61</sup>

In the present work, we apply this method to investigate the folding response of an immobilized 15-mer thrombin-binding DNA aptamer, its conformations in solutions of different

metal-ion composition, and how these metal ions impact changes in conformation upon binding of its target, alpha-thrombin. The thrombin-binding aptamer (TBA) is a guanine-rich sequence that forms a pair of stacked anti-parallel G-quadruplexes in the presence of stabilizing cations (potassium and sodium) while in lithium-ion solutions the aptamer remains in an unfolded state. 30,62,63 High-resolution crystal structures of the thrombin-TBA complex crystallized in the presence of sodium or potassium ions show the aptamer in a G-quadruplex conformation bound to its target protein.<sup>64</sup> The influence of metal-cation solution composition on immobilized-aptamer conformation upon binding of thrombin is an interesting question. The electrochemical response of a redox-modified TBA indicates that in low ionic-strength solutions, thrombin can induce folding of the aptamer generating a two-fold greater response than at high ionic strengths where the aptamer is already folded even in the absence of thrombin. 65 Because aptamer-based biosensors generally rely on conformation changes for read-out, it is valuable to have spectroscopic information of aptamer structure to help interpret the origins of their response. Using confocal-Raman microscopy, therefore, we determine the conformations of immobilized TBA while varying the metal-cation solution composition, quantifying the fraction of aptamer in G-quadruplex form from the vibrational frequencies and intensities of its Raman scattering. Association of alphathrombin with the immobilized aptamer can also be detected in Raman scattering from bound protein. Conformation changes in the aptamer upon binding of thrombin from solutions containing either lithium or potassium ions are compared, which allows one to quantify how binding of alphathrombin impacts folding of the aptamer under these conditions.

#### **EXPERIMENTAL SECTION**

Reagents and materials. Spherical chromatographic silica particles were purchased from YMC America (Devens, MA) with an average particle diameter of 5-um, a pore diameter of 31-nm, and a specific surface area of 117 m<sup>2</sup>/g, as specified by the manufacturer. The thrombin-binding aptamer with a 5' disulfide group was prepared by solid-phase synthesis at the University of Utah DNA Synthesis Facility, using the 5'-hexyl disulfide-phosphoramidite modifier (C6 SS) from Glen Research (Sterling, VA). DNA sequences were the 15-mer thrombin-binding aptamer with a 5' T9 spacer and disulfide linker: (C6 SS)-5'-TTT TTT TTT GGT TGG TGT GGT TGG-3', an equivalent TBA sequence having a 5' T<sub>16</sub> spacer for immobilization, a 15-mer complement to the TBA sequence: 5'-CCA ACC ACA CCA ACC-3', and a 15-mer control whose 3' terminus is a

sequence that has been shown not to bind thrombin,<sup>25</sup> (C6 SS)-5'-TTT TTT TTT GGT GGT GGT TGT GGT -3'. Standard reagents are listed in Supporting Information.

Thiol functionalization of silica. Functionalization of porous silica particles with thiol groups has been previously described.<sup>59</sup> Briefly, a 20-mg sample of silica particles was washed with acid piranha (Caution: corrosive, strong oxidizer, can react explosively with organics) to remove carbon-based contaminants. Particles were then rinsed twice by centrifugation and resuspension with deionized water and ethanol, and five-times in anhydrous dichloromethane (DCM). Particles were suspended in DCM and then reacted with 2,2-dimethoxy-1-thia-2-silcyclopentane for 1 hour. Excess silane was quenched with ethanol, and the sample washed with ethanol and deionized water. Particles were stored in deionized water at 2°C and were stable for months.

Coupling thiol-DNA to the thiolated silica surface. Samples of 5'-disulfide-conjugated DNA were prepared by the University of Utah DNA and Peptide Core Facility. As described in detail elsewhere, <sup>59</sup> the DNA-disulfide was reduced in a solution of 50-mM DTT, 1-mM EDTA, and 2% trimethylamine, and purified by precipitation upon addition of ethanol, followed by centrifugation and ethanol washing to remove excess DTT. The thiol-DNA was then reacted with >10-fold molar excess of 1,11-bismaleimido-triethyleneglycol in 50/50 DMF/Tris buffer pH 7.4 containing 200-mM NaCl and 500-μM TCEP. The maleimide-conjugated DNA was purified by precipitation by addition of ethanol (-20 C), centrifuged, and washed with ethanol, DMF, and ethanol. Ethanol was removed by evaporation, and the maleimide-conjugated DNA was rehydrated in aqueous 400-mM NaCl solution (not buffered) and reacted with thiol-functionalized silica particles for 12-hours. For producing full monolayer coverage of DNA, the rehydrated solution was diluted with an equal volume of DMF prior to reaction.<sup>59</sup>

Following the DNA functionalization, silica particles were washed 3-times with 95:5 DMF: pH 6.5 MES buffer. To backfill the remaining exposed surface with PEG, samples were reacted with 1 mg/ml PEG<sub>2000</sub>-maleimide in 95:5 DMF:pH 6.5 MES buffer for 12 hours. Note that a high-volume fraction of DMF is needed to prevent non-specific adsorption of PEG<sub>2000</sub> to the silica surface. Following reaction with PEG<sub>2000</sub>-maleimide, particle were washed in 150 mM LiCl pH 6.5 MES buffer and stored at 2°C for up to a week.

**Confocal Raman microscopy.** The confocal Raman microscope has been described in detail previously.<sup>66</sup> Briefly, a 647.1-nm Kr<sup>+</sup> laser beam is bandpass filtered, expanded, and directed into an inverted microscope (Nikon), reflected off a dichroic beam splitter, and directed into a 1.4-

NA, 100x oil-immersion objective, producing a ~600-nm diameter beam waist. Scattered light from the confocal probe volume is collected by the same objective, transmitted though the dichroic beam splitter, passed through a long pass filter (all Semrock), focused through the 50-µm slit of a 500-mm focal-length spectrograph (Bruker 500IS), and dispersed with a 300-line/mm grating, blazed at 762 nm. Raman scattering is imaged onto a charge-coupled-device detector (Andor).

Well cells for confocal Raman microscopy were constructed by gluing a ~12-mm length of 10-mm i.d., Pyrex tubing to a No. 1 glass coverslip with epoxy resin. To collect spectra, the beam was focused to the solution/coverslip interface, and the stage was adjusted in the x-, y-, and z-dimensions until the confocal probe volume was centered within a single particle. Reported spectra are the average of 1-min integrations collected from 12 individual particles. Spectra were truncated to the frequency region of interest and baseline corrected with a rolling-circle algorithm.<sup>67</sup> Data analysis was carried out in Matlab (Mathworks, Natick, MA) using custom scripts.

#### RESULTS AND DISCUSSION

Aptamer immobilization to porous silica by thiol-maleimide Michael addition. To provide conformational freedom, the 15mer thrombin-binding aptamer was synthesized with a 9-thymine spacer and thiol-functional group at its 5' surface-proximal end. The aptamer was immobilized at sub-monolayer densities with a bismaleimide reagent that the thiolated **TBA** to thiolcouples functionalized silica surfaces.<sup>59</sup> Briefly, thiolated-TBA undergoes a Michael-addition reaction with a large excess of bismaleimide, producing a maleimide-linker conjugated to the through a succinimide bond. aptamer Following removal of excess bismaleimide, the

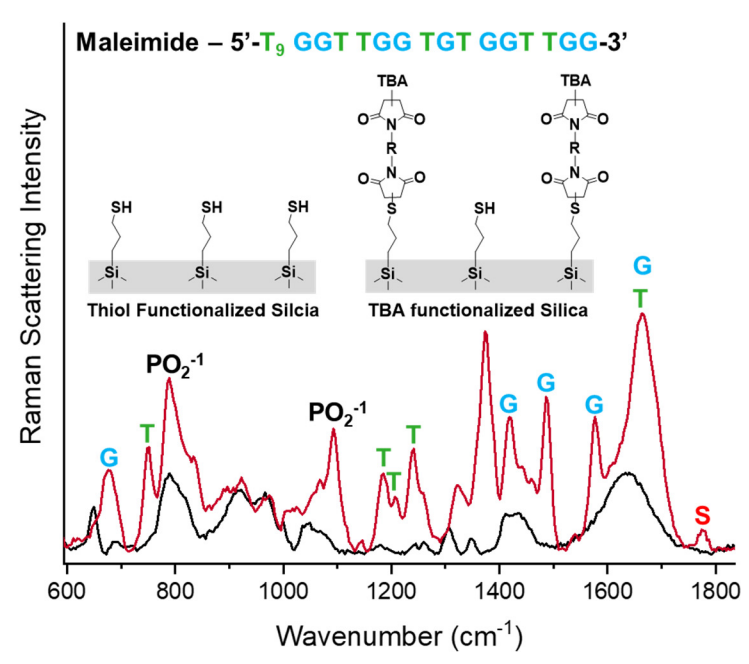


Figure 1. Immobilization of 15-mer thrombin-binding aptamer to porous silica with thiol-maleimide Michael-addition chemistry. Raman spectra of thiol-functionalized silica prior to (black) and following reaction with maleimide-conjugated DNA (red).

maleimide-conjugated DNA is covalently bonded to the thiolated-silica surface via second Michael-addition reaction (Experimental Section).

To verify immobilization of the TBA, confocal-Raman spectroscopy was used to characterize the thiol-functionalized silica particles prior to and following DNA immobilization. The Raman spectrum (Figure 1) of thiol-functionalized silica shows SiO<sub>2</sub> stretching modes (750 – 1000 cm<sup>-1</sup>), a water bend (1650 cm<sup>-1</sup>), along with C-C stretching and CH<sub>2</sub> twisting and bending modes (1025–1500 cm<sup>-1</sup>). Thiol-functionalized particles reacted with the maleimide-DNA conjugate exhibit Raman scattering from both DNA and succinimide bonds formed by thiol-maleimide reactions attaching DNA to the surface (Figure 1). Scattering from the succinimide stretch at 1770 cm<sup>-1</sup> verifies the surface-coupling chemistry and serves as a convenient internal standard for normalizing spectra.

When calibrated against a phenyl-maleimide standard, immobilized with the same succinimide bond and whose coverage is determined by elemental carbon analysis,<sup>59</sup> the succinimide-scattering intensity of the immobilized TBA can be used to quantify its absolute surface-density (details in Supporting Information). Using this approach, we determined the submonolayer coverage of immobilized TBA to be  $\Gamma_{TBA} = 110 \pm 20 \text{ nmol/m}^2$ , which corresponds to a root-mean-squared distance between aptamers of  $3.9 \pm 0.7 \text{ nm}$ . To avoid non-specific surface interactions with the target protein, a backfilling step with PEG<sub>2000</sub>-maleimide was performed following DNA immobilization (Experimental Section). The surface-density of PEG,  $\Gamma_{PEG} = 140 \pm 20 \text{ nmol/m}^2$  (~30% greater than TBA) was determined from the subsequent increase in succinimide scattering (Supporting Information).

## Quantifying metal ion-dependent conformations of the thrombin-binding aptamer.

The 15-mer thrombin-binding aptamer is a short, guanine-rich sequence of single-stranded DNA capable of adopting a stacked pair of anti-parallel G-quadruplexes, each of which consists of four guanine bases that form a tetrad arrangement stabilized by non-canonical intramolecular Hoogsteen base-pairing (Figure S3, Supporting Information). The functionality of the aptamer is to bind the serum protein alpha-thrombin, which is reported to depend on the aptamer forming a G-quadruplex structure. The stability of G-quadruplexes has been shown to be sensitive to the metal cations present in solution. Potassium and sodium stabilize G-quadruplex formation, whereas lithium has been reported to have negligible stabilizing effects. Part of the challenge in predicting the folding of an aptamer like 15-mer TBA is that its conformation may be stabilized by both interactions with the target analyte and by metal cations in solution. The goal of this work is, therefore, to elucidate how specific metal cations govern conformations of the surface-immobilized thrombin aptamer and how these conformations

may change upon association with alpha-thrombin. In addition, our goal is to establish new methodology capable of assessing conformations of aptamers at interfaces upon binding of their protein targets.

To investigate conformations of TBA in the presence of stabilizing and non-stabilizing metal-cations composition, aptamer-functionalized particles were suspended in pH-6.5 MES

buffers, containing either 150-mM LiCl or 150-mM KCl. Raman spectra from the immobilized aptamer were acquired and plotted in Figure 2, along with a difference spectrum. Labeled in difference spectrum are the cation-dependent changes in frequency and intensity of the aptamer vibrational modes. In the presence of K<sup>+</sup> (relative to Li<sup>+</sup>), the 686 cm<sup>-1</sup> guanine ring stretch associated with the C2'endo/anti conformation signifishifts, cantly narrows, and

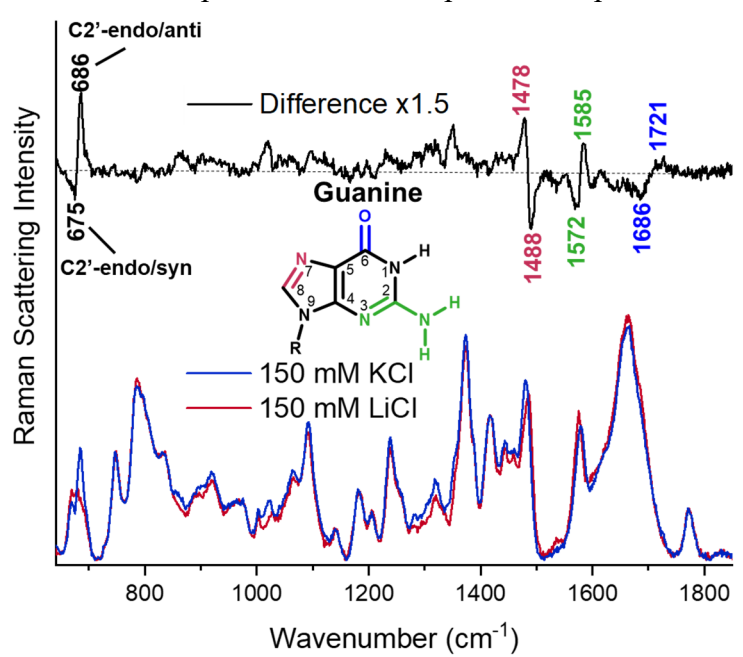


Figure 2. Raman spectrum of surface-immobilized thrombin-binding aptamer in 150-mM LiCl (red) and 150-mM KCl (blue). Difference spectrum (black) highlights ion-dependent changes.

increases in intensity, suggesting a more ordered structural conformation: consistent with G-quadruplex formation. Additionally, there are changes in the frequency of several guanine-related vibrational modes that are sensitive to base-pairing. In the presence of K<sup>+</sup> (relative to Li<sup>+</sup>), the 1488 cm<sup>-1</sup> C8=N7 coupled band shifts to 1478 cm<sup>-1</sup>, the 1572 cm<sup>-1</sup> C2=N3 coupled band shifts to 1585 cm<sup>-1</sup> and the 1686 cm<sup>-1</sup> carbonyl stretch at C6 shifts to 1721 cm<sup>-1</sup>. All these spectral differences are associated with the formation of Hoogsteen base-pairs that stabilize the G-quadruplex structure (Figure S3), indicating that the aptamer is unfolded in Li<sup>+</sup> and folds to a G-quadruplex conformation when stabilized by K<sup>+</sup>.

These results demonstrate that Raman scattering can detect ion-dependent conformational changes in the thrombin-binding aptamer. To investigate how the populations of aptamer conformations respond to varying concentrations of stabilizing K<sup>+</sup> cations, Raman spectra were acquired of immobilized TBA particles suspended in solutions having varying concentrations of K<sup>+</sup> at constant ionic strength (150 mM) maintained by adjusting Li<sup>+</sup>; the results are presented in

Figure 3A. Because there is no established model for TBA folding in response to K<sup>+</sup> concentration, a model-free analysis, self-modeling curve resolution (SMCR), was employed to obtain a detailed picture of the observed spectral changes. SMCR is a multivariate statistical method that resolves correlated changes in a series of spectra across a variation in composition by eigenvector decomposition of the variance-covariance matrix of the data (Supporting Information).<sup>72-75</sup> The pure component spectra and corresponding composition vectors that describe the data are

determined from linear combinations of the eigenvectors, subject to nonnegativity constraints on the spectral intensities and component amplitudes (Supporting Information).

SMCR analysis identified two significant components, where the resolved pure-component spectra are plotted in Figure 3A, and the corresponding composition vectors (contributions of these two spectra versus K<sup>+</sup> concentration) are in Figure 3B. The quality of fit of data to the product of these component vectors (Figure S4) supports a key assumption in the analysis: that the aptamer exists in two distinct conformations, either folded or unfolded. The variation with K<sup>+</sup> concentration is therefore not an evolution through partially folded forms, but an equilibrium between two states represented by the purecomponent spectra.

From the results in Figure 3B, the fraction of the unfolded aptamer in a pure Li<sup>+</sup> buffer is found to be

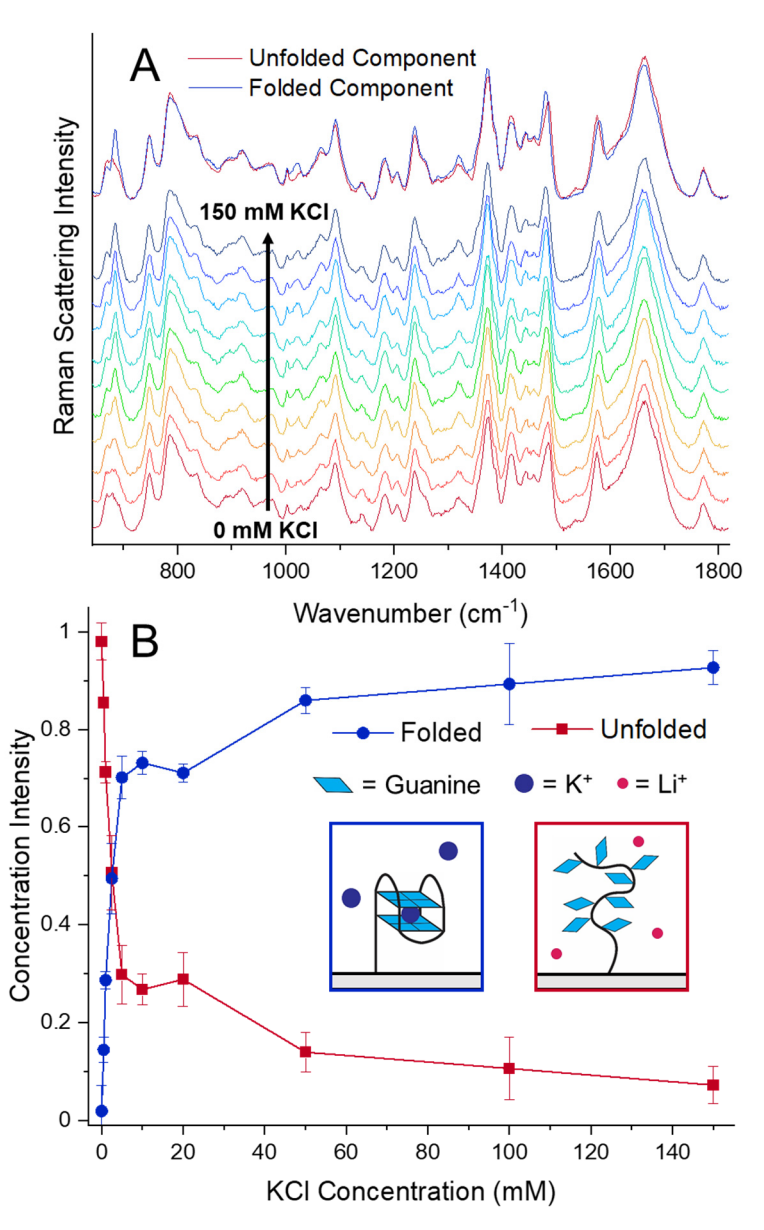


Figure 3. (A) Raman spectra of surface-immobilized TBA in solutions of varying KCl concentration. Top spectra show pure-component folded and unfolded spectra from self-modeling-curve resolution. (B) Component concentrations from SMCR analysis versus KCl concentration.

 $0.98\pm0.04$ , indicating that the immobilized aptamer exhibits no measurable G-quadruplex conformer in the absence of potassium ion. With addition of  $K^+$ , the fraction of folded aptamer increases with a steep dependence on  $K^+$  concentration followed by a gradual rollover, indicating that relatively small concentrations of  $K^+$  stabilize the G-quadruplex conformation of the aptamer. This finding is consistent with previous NMR studies of the 15-mer thrombin-binding aptamer, which showed that the aptamer in solution requires a minimal concentration ( $\gtrsim 1$ -mM) of potassium ion to form detectable anti-parallel G-quadruplex conformation. As the  $K^+$  concentration increases to 150 mM, the fraction of the aptamer population in the G-quadruplex conformation is  $0.93\pm0.04$ , indicating that the aptamer population retains a small ( $0.07\pm0.04$ ) but measurable fraction of the unfolded form in its Raman spectrum. This small unfolded fraction may arise from local steric constraints or surface interactions that arise from immobilization of the aptamer to the silica surface.

TBA conformational changes upon binding of thrombin. By quantifying the relative population of conformations adopted by the aptamer in the presence of the two metal cations, we now determine whether alpha-thrombin binds to the immobilized aptamer. We also seek to discover whether alpha-thrombin can actively bind to the aptamer in the absence of the stabilizing K<sup>+</sup> cation, and if so, whether this binding is accompanied with conformational changes in the aptamer. A crucial issue in this experiment is to ensure that any scattering from alpha-thrombin binding is due to its selective binding with the aptamer and not a consequence of non-specific association with the surrounding surface. To assess the selectivity of alpha-thrombin-binding, we first prepared control samples that were equilibrated with a high concentration (50-μM) solution of a 15-mer complement sequence. The formation of a hybridized DNA duplex with the aptamer is expected to disrupt the G-quadruplex conformation associated with thrombin binding.<sup>64</sup> The efficiencies of aptamer hybridization were determined from the relative changes in the phosphate stretching mode at 1094 cm<sup>-1</sup> with addition of 50-μM complement and found to be 95±8% and

98±8% in LiCl and KCl buffers, respectively, consistent with complete duplex formation (details

in Supporting Information).

To investigate the selectivity of thrombin binding to the immobilized aptamer, samples of particles in 150-mM LiCl and KCl pH 6.5 MES buffer, respectively, were prepared with and without 50µM 15-mer complement DNA and equilibrated for ~12-hours. Samples were then characterized prior to and following the equilibration with 500nM alpha-thrombin, and the results are plotted in Figure 4. Each pair of spectra in Figure 4A shows the impact of equilibration with alphathrombin in KCl buffer, where red spectra indicate alpha-thrombin interaction with the folded aptamer, and the cyan spectra are for the control sample where the aptamer is hybridized with 15-mer its complement. As can be observed in the black difference spectra, equilibration of alpha-thrombin reveals a much greater increase in scattering with the folded aptamer compared to the hybridized control.

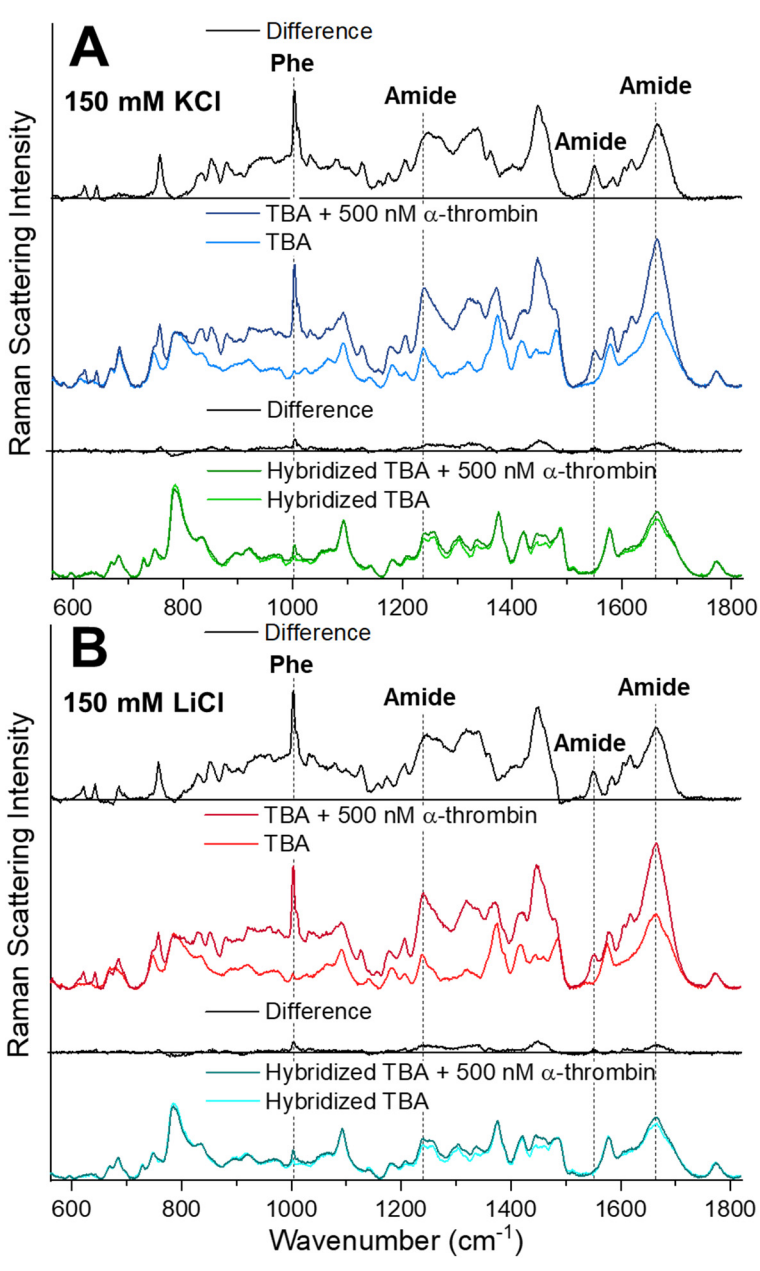


Figure 4. Raman spectra of TBA-particles before (lighter) and after (darker) equilibration with alpha-thrombin. Difference spectra are in black. (A) TBA in KCl (blue). Hybridized-TBA control in KCl (cyan). (B) TBA in LiCl (red). Hybridized-TBA control in LiCl (green).

Specific evidence of protein accumulation in the former is found in the band frequencies characteristic of amino acid residues and the amide backbone.<sup>78</sup> For example, the appearance of tryptophan (757, 880, 1335 cm<sup>-1</sup>) phenylalanine (1004 and 1031 cm<sup>-1</sup>), tyrosine (642, 830 and 850 cm<sup>-1</sup>), aliphatic amino acid (1332 and 1446 cm<sup>-1</sup>), and amide backbone modes (1250, 1550, 1664

cm<sup>-1</sup>) are consistent with protein band assignments.<sup>78</sup> Given these bands in the difference spectrum, we can conclude that alpha-thrombin has accumulated within the TBA-derivatized particles.

To determine what fraction of thrombin binding is a due to selective interactions with the folded aptamer, we compare the protein band intensities to those observed with alpha-thrombin interacting with a hybridized dsDNA aptamer control, where G-quadruplex formation is inhibited. The scattering intensity from protein in the control sample is 7.8±0.8% of the thrombin intensity observed for binding to the folded aptamer. This fraction is not due displacement of the DNA complement from the aptamer since none of the spectral intensity from the 15-mer complement is lost following the addition of alpha-thrombin. We conclude that the majority (>92%) of the alphathrombin captured by the folded aptamer arises from selectively bound protein. The selectivity is further tested by comparing the binding of alpha-thrombin to a modified 3'terminal sequence having the same base composition, but with a sequence that was previously shown in an electrochemical aptamer sensor experiment not to bind thrombin.<sup>25</sup> The results (Supporting Information) show no detectable thrombin association with this control sequence compared with the 15-mer TBA, which exhibits strong thrombin binding. In addition, thrombin binding to the immobilized TBA is reversible, where bound thrombin can be displaced from the aptamer by exposing the thrombin-aptamer complex to 50-µM complement DNA (Supporting Information). Finally, unlike SERS measurements of DNA immobilized on plasmonic metals, 57,58 the measured alpha-thrombin capture response should not decay with distance from the surface. An experiment to test this issue was carried out, where thrombin binding to the 15-mer TBA immobilized through a 15-T spacer and the results are plotted in Figure S7 (Supporting Information). The Raman scattering from the captured alpha-thrombin upon exposure to 500-nM thrombin in solution exhibits signal strengths that are equivalent to those observed with the shorter 9-T tether in Figure 4 above.

Having established that alpha-thrombin binds selectively and reversibly to the folded aptamer in the presence of a G-quadruplex-stabilizing potassium ion, we now test whether alpha-thrombin can bind to an initially unfolded aptamer. In Figure 4B, we present results of an equivalent experiment, except where the thrombin association with the immobilized aptamer occurs in 150-mM LiCl buffer. The spectra in blue (and the difference spectrum above them) show that alpha-thrombin binds selectively to the initially unfolded aptamer in Li<sup>+</sup> solution, where only

a small background is observed for thrombin association with the hybridized control in green. To determine whether protein binding by the aptamer in  $Li^+$  solution changes its conformation to a G-quadruplex form, we focus our analysis on a region containing a guanine-ring stretching mode  $(650 - 715 \text{ cm}^{-1})$  that was shown in the previous section to be informative of G-quadruplex formation, a band that is unobscured by overlapping protein scattering intensity. High-resolution

Raman spectra (Figure 5A) reveal that in the presence of KCl, there are no spectral differences in the aptamer conformation upon protein binding, which is consistent with the aptamer being folded both prior to and after association with alpha-thrombin. In contrast, the binding of alpha-thrombin to the aptamer in LiCl shows significant changes in intensity of the guanine mode following binding. These spectral changes are consistent with a conformation change (folding) of the aptamer upon binding of alpha-thrombin, stabilizing the folded G-quadruplex structure, which in agreement with equivalent conclusions drawn from the 2-fold greater electrochemical response at low ionic strengths of a 31-mer TBA having the same 15-mer sequence at its 3' terminus.65

To quantify the fraction of the surface-immobilized aptamer that folds following the interaction with alpha-thrombin, we apply a least-squares analysis to fit the guanine ring stretching band to the two pure component spectra determined from the K<sup>+</sup> concentration dependence in the previous section. The results of this analysis in Figure 5B show that,

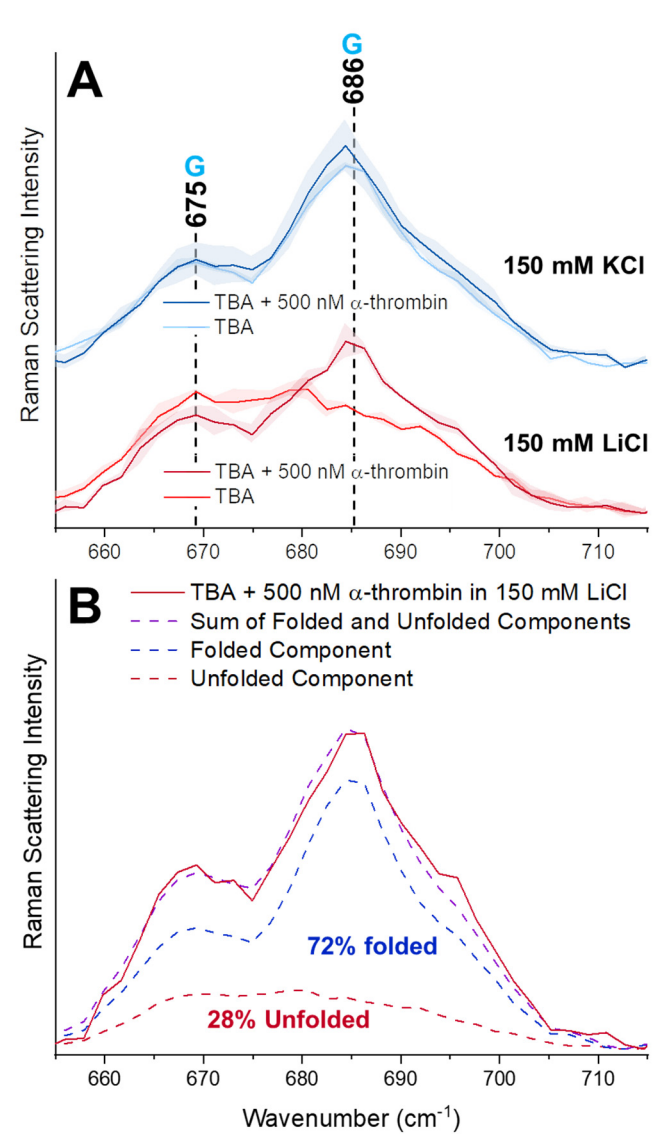


Figure 5. Raman spectra of the guanine ring-stretching mode. (A) Spectra before (lighter) and after (darker) reaction with 500-nM alpha-thrombin in KCl (blue) or in LiCl (red); the y-axis of the KCl results has been offset to allow clearer comparison of the results. (B) Least-squares fit of spectral components from SMCR analysis to quantify folded and unfolded fractions of TBA following reaction in 150-mM LiCl.

upon binding alpha-thrombin in LiCl buffer, 72% of the immobilized aptamer is in the folded G-

quadruplex conformation, while 28% of the aptamer remains unfolded. A simple explanation for incomplete folding of the immobilized aptamer is that the surface-density of aptamers on the silica surface exceeds the maximum density of thrombin that can accumulate at the interface, limiting the ability of some of the immobilized aptamers to bind alpha-thrombin. While the 15-mer TBA has been shown to have 2 binding sites for alpha-thrombin in free solution, <sup>79-82</sup> only one of these sites is accessible to alpha-thrombin binding when the aptamer is immobilized at an interface. <sup>23</sup> Thus a close-packed monolayer of alpha-thrombin would correspond to the maximum population of aptamer that can be bound to protein.

The maximum surface-density of alpha-thrombin can be estimated from the crystalstructure of the alpha-thrombin/aptamer complex<sup>64</sup> and then compared to the surface-population of the folded aptamer quantified above. Based on the size of alpha-thrombin in its orientation relative to a surface-immobilized aptamer (Supporting Information),<sup>64</sup> a closely-packed thrombin monolayer would have a surface-density of 86 nmol/m<sup>2</sup>. This thrombin surface-density can be compared with the density of aptamer in a G-quadruplex conformation following its binding with alpha-thrombin,  $\Gamma_{folded\ TBA} = 0.72\ \Gamma_{TBA} = 79\ (\pm 14)\ nmol/m^2$ . The surface-density of folded aptamer population agrees, within its uncertainty, with the packing density of alpha-thrombin monolayer, indicating that 28% of aptamers remain unfolded due to alpha-thrombin having reached a maximum surface-coverage leaving excess unbound aptamer. This analysis can only be accomplished with a LiCl buffer, where the change in conformation of the aptamer accompanies binding of its protein target. Note there is a limit to the immobilized TBA surface density that will allow alpha-thrombin binding. Saturation coverage of DNA was accomplished by carrying out the maleimide-thiol coupling reaction in 50% DMF.<sup>59</sup> where the immobilized TBA surface density is 4-times greater than above,  $\sim$ 460( $\pm$ 90) nmol/m<sup>2</sup>. This corresponds to a root-mean-square distance between immobilized DNA molecules of 1.9(±0.2) nm, comparable to the size of the folded aptamer (Figure S8). Under these conditions, we detect strong Raman-scattering from the immobilized DNA (Figure S9). However, the capture of alpha-thrombin is greatly reduced, because the close spacing of immobilized TBA allows only a fraction of the aptamers to form antiparallel G-quadruplexes, which in turn lowers thrombin binding. A systematic study of the surfacedensity dependence of TBA-protein association is underway in our lab.

**Conclusions.** In this work, we have adapted *in-situ* Raman spectroscopy to determine how the association of a surface-immobilized aptamer with its protein target impacts the aptamer conformation. Raman scattering reports binding of the protein, and more importantly, is

informative of aptamer conformations. The results revealed that in the presence of K<sup>+</sup> ion, the immobilized aptamer is in a G-quadruplex form both before and after binding of thrombin. This finding is contrary to an interpretation of the electrochemical response of this aptamer with K<sup>+</sup> present in solution, which suggested that formation of the G-quaduplex upon thrombin-binding inhibited access of the aptamer redox-label to the electrode surface.<sup>25</sup> Based on the results presented here, it is likely instead that the size of the bound thrombin (Figure S5) obstructed access of the redox-label to the electrode. For experiments in Li<sup>+</sup> solution, Raman scattering showed the aptamer changes from an unfolded to a folded state upon binding of its protein target. These results also showed that the fraction of surface-immobilized aptamers in a folded state is limited by the size of the bound protein and its packing density.

This study represents an advancement in experimental technique to understand surface-immobilized aptamers and factors that influence their conformations and reactivity. While the present study focused on an aptamer with G-quadruplex secondary structure, the methodology could also be applied to aptamers that undergo hybridization changes in stem-loop regions upon analyte binding, where Raman-scattering changes upon duplex formation are readily detected and interpreted. Future applications would include measuring binding isotherms while identifying sites of interaction between the aptamer and its target through shifts in vibrational frequencies and intensities, as recently demonstrated for small-molecule binding to dsDNA. In addition to investigations of biosensors, this method would allow studies of the association of proteins with specific sequences of double-stranded DNA or modified DNA bases. Examples would include studies of selective binding of repair enzymes to sequences that include oxidized bases, 48,85 or proteins that recognize DNA methylation and thereby regulate transcription. For the present results, therefore, set a precedent for future research that requires an understanding of structure-function relationships in protein interactions with oligonucleotides bound to surfaces.

#### ASSOCIATED CONTENT

## **Supporting Information.**

Additional information on standard reagent sources, backfilling with PEG, quantifying surface density of TBA and PEG, structure of the G-quadruplex, self-modeling curve resolution of folded versus unfolded TBA, quantification of hybridization efficiency of TBA, testing the sequence selectivity, reversibility, tether-length and surface-density dependence of alpha-thrombin binding, dimensions of alpha-thrombin/aptamer complex, and references.

### **ACKNOWLEDGEMENTS**

This work was supported by the National Science Foundation under Grant CHE-1904424 and from the U.S. Department of Energy, Office of Basic Energy Sciences under Grant DE-FG03-93ER14333. The authors are grateful to W. Mike Hanson of the University of Utah Core DNA Synthesis Facility for contributions to this project.

#### REFERENCES

- (1) Liu, J.; Cao, Z.; Lu, Y. Functional Nucleic Acid Sensors. *Chem. Rev.* **2009**, *109*, 1948-1998.
- (2) Mirkin, C.A.; Letsinger, R.L.; Mucic, R.C.; Storhoff, J.J. A DNA-based method for rationally assembling nanoparticles into macroscopic materials. *Nature* **1996**, *382*, 607-609.
- (3) Sontakke, V.A.; Yokobayashi, Y. Programmable Macroscopic Self-Assembly of DNA-Decorated Hydrogels. *J. Am. Chem. Soc.* **2022**, *144*, 2149-2155.
- (4) Keefe, A.D.; Pai, S.; Ellington, A. Aptamers as therapeutics. *Nat. Rev. Drug Discovery* **2010**, *9*, 537-550.
- (5) Rothemund, P.W.K. Folding DNA to create nanoscale shapes and patterns. *Nature* **2006**, 440, 297-302.
- (6) Michaud, M.; Jourdan, E.; Villet, A. et al. A DNA Aptamer as a New Target-Specific Chiral Selector for HPLC. J. Am. Chem. Soc. 2003, 125, 8672-8679.
- (7) Ellington, A.D.; Szostak, J.W. Selection in vitro of single-stranded DNA molecules that fold into specific ligand-binding structures. *Nature* **1992**, *355*, 850-852.
- (8) Ellington, A.D.; Szostak, J.W. In vitro selection of RNA molecules that bind specific ligands. *Nature* **1990**, *346*, 818-822.
- (9) Hermann, T.; Patel, D.J. Adaptive Recognition by Nucleic Acid Aptamers. *Science* **2000**, 287, 820-825.
- (10) Bock, L.C.; Griffin, L.C.; Latham, J.A.; Vermaas, E.H.; Toole, J.J. Selection of single-stranded DNA molecules that bind and inhibit human thrombin. *Nature* **1992**, *355*, 564-566.
- (11) Yang, Q.; Goldstein, I.J.; Mei, H.-Y.; Engelke, D.R. DNA ligands that bind tightly and selectively to cellobiose. *Proc. Natl. Acad. Sci. U. S. A.* **1998**, *95*, 5462-5467.
- (12) Huizenga, D.E.; Szostak, J.W. A DNA Aptamer That Binds Adenosine and ATP. *Biochemistry* **1995**, *34*, 656-665.
- (13) Morris, F.D.; Peterson, E.M.; Heemstra, J.M.; Harris, J.M. Single-Molecule Kinetic Investigation of Cocaine-Dependent Split-Aptamer Assembly. *Anal. Chem.* **2018**, *90*, 12964 12970.
- (14) Kammer, M.N.; Kussrow, A.; Gandhi, I.*et al.* Quantification of Opioids in Urine Using an Aptamer-Based Free-Solution Assay. *Anal. Chem.* **2019**, *91*, 10582-10588.
- (15) Reese, C.B. Oligo- and poly-nucleotides: 50 years of chemical synthesis. *Org. Biomol. Chem.* **2005**, *3*, 3851.

- (16) Thiviyanathan, V.; Gorenstein, D.G. Aptamers and the next generation of diagnostic reagents. *PROTEOMICS Clinical Applications* **2012**, *6*, 563-573.
- (17) Li, Y.; Liu, J. Aptamer-based strategies for recognizing adenine, adenosine, ATP and related compounds. *Analyst* **2020**, *145*, 6753-6768.
- (18) Jhaveri, S.D.; Kirby, R.; Conrad, R.et al. Designed Signaling Aptamers that Transduce Molecular Recognition to Changes in Fluorescence Intensity. J. Am. Chem. Soc. **2000**, 122, 2469-2473.
- (19) Wu, Y.; Ranallo, S.; Del Grosso, E.et al. Using Spectroscopy to Guide the Adaptation of Aptamers into Electrochemical Aptamer-Based Sensors. *Bioconjugate Chem.* **2023**, *34*, 124-132.
- (20) Deng, B.; Lin, Y.; Wang, C.et al. Aptamer binding assays for proteins: The thrombin example—A review. *Anal. Chim. Acta* **2014**, *837*, 1-15.
- (21) Xia, T.; Yuan, J.; Fang, X. Conformational Dynamics of an ATP-Binding DNA Aptamer: A Single-Molecule Study. *J. Phys. Chem. B* **2013**, *117*, 14994-15003.
- (22) Mashima, T.; Matsugami, A.; Nishikawa, F.; Nishikawa, S.; Katahira, M. Unique quadruplex structure and interaction of an RNA aptamer against bovine prion protein. *Nucleic Acids Res.* **2009**, *37*, 6249-6258.
- (23) Lin, P.-H.; Chen, R.-H.; Lee, C.-H.et al. Studies of the binding mechanism between aptamers and thrombin by circular dichroism, surface plasmon resonance and isothermal titration calorimetry. *Colloids Surf.*, B **2011**, 88, 552-558.
- (24) Nagatoishi, S.; Tanaka, Y.; Tsumoto, K. Circular dichroism spectra demonstrate formation of the thrombin-binding DNA aptamer G-quadruplex under stabilizing-cation-deficient conditions. *Biochem. Biophys. Res. Commun.* **2007**, *352*, 812-817.
- (25) Xiao, Y.; Lubin, A.A.; Heeger, A.J.; Plaxco, K.W. Label-Free Electronic Detection of Thrombin in Blood Serum by Using an Aptamer-Based Sensor. *Angew. Chem.* **2005**, *117*, 5592-5595.
- (26) Xiao, Y.; Qu, X.; Plaxco, K.W.; Heeger, A.J. Label-Free Electrochemical Detection of DNA in Blood Serum via Target-Induced Resolution of an Electrode-Bound DNA Pseudoknot. *J. Am. Chem. Soc.* **2007**, *129*, 11896-11897.
- (27) Nagatoishi, S.; Nojima, T.; Galezowska, E.; Juskowiak, B.; Takenaka, S. G Quadruplex-Based FRET Probes with the Thrombin-Binding Aptamer (TBA) Sequence Designed for the Efficient Fluorometric Detection of the Potassium Ion. *ChemBioChem* **2006**, *7*, 1730-1737.

- (28) Baker, B.R.; Lai, R.Y.; Wood, M.S.*et al.* An Electronic, Aptamer-Based Small-Molecule Sensor for the Rapid, Label-Free Detection of Cocaine in Adulterated Samples and Biological Fluids. *J. Am. Chem. Soc.* **2006**, *128*, 3138-3139.
- (29) Reinstein, O.; Yoo, M.; Han, C.*et al.* Quinine Binding by the Cocaine-Binding Aptamer. Thermodynamic and Hydrodynamic Analysis of High-Affinity Binding of an Off-Target Ligand. *Biochemistry* **2013**, *52*, 8652-8662.
- (30) Ponzo, I.; Möller, F.M.; Daub, H.; Matscheko, N. A DNA-Based Biosensor Assay for the Kinetic Characterization of Ion-Dependent Aptamer Folding and Protein Binding. *Molecules* **2019**, *24*, 2877.
- (31) Kankia, B.I.; Marky, L.A. Folding of the Thrombin Aptamer into a G-Quadruplex with Sr<sup>2+</sup>: Stability, Heat, and Hydration. *J. Am. Chem. Soc.* **2001**, *123*, 10799-10804.
- (32) Macaya, R.F.; Schultze, P.; Smith, F.W.; Roe, J.A.; Feigon, J. Thrombin-binding DNA aptamer forms a unimolecular quadruplex structure in solution. *Proc. Natl. Acad. Sci. U. S. A.* **1993**, *90*, 3745-3749.
- (33) Bottari, F.; Daems, E.; De Vries, A.-M.*et al.* Do Aptamers Always Bind? The Need for a Multifaceted Analytical Approach When Demonstrating Binding Affinity between Aptamer and Low Molecular Weight Compounds. *J. Am. Chem. Soc.* **2020**, *142*, 19622-19630.
- (34) Idili, A.; Gerson, J.; Kippin, T.; Plaxco, K.W. Seconds-Resolved, In Situ Measurements of Plasma Phenylalanine Disposition Kinetics in Living Rats. *Anal. Chem.* **2021**, *93*, 4023-4032.
- (35) Parolo, C.; Idili, A.; Ortega, G.et al. Real-Time Monitoring of a Protein Biomarker. ACS Sens. 2020, 5, 1877-1881.
- (36) Sykes, K.S.; Oliveira, L.F.L.; Stan, G.; White, R.J. Electrochemical Studies of Cation Condensation-Induced Collapse of Surface-Bound DNA. *Langmuir* **2019**, *35*, 12962-12970.
- (37) Watkins, H.M.; Vallée-Bélisle, A.; Ricci, F.; Makarov, D.E.; Plaxco, K.W. Entropic and Electrostatic Effects on the Folding Free Energy of a Surface-Attached Biomolecule: An Experimental and Theoretical Study. *J. Am. Chem. Soc.* **2012**, *134*, 2120-2126.
- (38) Watkins, H.M.; Simon, A.J.; Ricci, F.; Plaxco, K.W. Effects of Crowding on the Stability of a Surface-Tethered Biopolymer: An Experimental Study of Folding in a Highly Crowded Regime. *J. Am. Chem. Soc.* **2014**, *136*, 8923-8927.
- (39) Brewer, S.H.; Anthireya, S.J.; Lappi, S.E.; Drapcho, D.L.; Franzen, S. Detection of DNA Hybridization on Gold Surfaces by Polarization Modulation Infrared Reflection Absorption Spectroscopy. *Langmuir* **2002**, *18*, 4460-4464.

- (40) Saprigin, A.V.; Thomas, C.W.; Dulcey, C.S.; Patterson, C.H.; Spector, M.S. Spectroscopic quantification of covalently immobilized oligonucleotides. *Surf. Interface Anal.* **2005**, *37*, 24-32.
- (41) Liao, W.; Wei, F.; Liu, D.et al. FTIR-ATR detection of proteins and small molecules through DNA conjugation. Sens. Actuators, B 2006, 114, 445-450.
- (42) Ho, J.-J.; Skoff, D.R.; Ghosh, A.; Zanni, M.T. Structural Characterization of Single-Stranded DNA Monolayers Using Two-Dimensional Sum Frequency Generation Spectroscopy. *J. Phys. Chem. B* **2015**, *119*, 10586-10596.
- (43) Boman, F.C.; Gibbs-Davis, J.M.; Heckman, L.M.et al. DNA at Aqueous/Solid Interfaces: Chirality-Based Detection via Second Harmonic Generation Activity. *J. Am. Chem. Soc.* **2009**, 131, 844-848.
- (44) Stokes, G.Y.; Gibbs-Davis, J.M.; Boman, F.C.*et al.* Making "Sense" of DNA. *J. Am. Chem. Soc.* **2007**, *129*, 7492-7493.
- (45) Perets, E.A.; Olesen, K.B.; Yan, E.C.Y. Chiral Sum Frequency Generation Spectroscopy Detects Double-Helix DNA at Interfaces. *Langmuir* **2022**, *38*, 5765-5778.
- (46) Benevides, J.M.; Overman, S.A.; Thomas, G.J. Raman, polarized Raman and ultraviolet resonance Raman spectroscopy of nucleic acids and their complexes. *J. Raman Spectrosc.* **2005**, *36*, 279-299.
- (47) Benevides, J.M.; Kawakami, J.; Thomas, G.J. Mechanisms of drug-DNA recognition distinguished by Raman spectroscopy. *J. Raman Spectrosc.* **2008**, *39*, 1627-1634.
- (48) Miura, T.; Thomas, G.J. Structural Polymorphism of Telomere DNA: Interquadruplex and Duplex-Quadruplex Conversions Probed by Raman Spectroscopy. **1994**, *33*, 7848-7856.
- (49) Benevides, J.M.; Chan, G.; Lu, X.-J.et al. Protein-Directed DNA Structure. I. Raman Spectroscopy of a High-Mobility-Group Box with Application to Human Sex Reversal†. *Biochemistry* **2000**, *39*, 537-547.
- (50) Movileanu, L.; Benevides, J.M.; Thomas, G.J. Temperature dependence of the raman spectrum of DNA. II. Raman signatures of premelting and melting transitions of poly(dA)·poly(dT) and comparison with poly(dA-dT)·poly(dA-dT)\*. *Biopolymers* **2002**, *63*, 181-194.
- (51) Neumann, O.; Zhang, D.; Tam, F.et al. Direct Optical Detection of Aptamer Conformational Changes Induced by Target Molecules. *Anal. Chem.* **2009**, *81*, 10002-10006.

- (52) Pagba, C.V.; Lane, S.M.; Wachsmann-Hogiu, S. Raman and surface-enhanced Raman spectroscopic studies of the 15-mer DNA thrombin-binding aptamer. *J. Raman Spectrosc.* **2010**, *41*, 241-247.
- (53) Pagba, C.; Lane, S.; Cho, H.; Wachsmann-Hogiu, S. Direct detection of aptamer-thrombin binding via surface-enhanced Raman spectroscopy. *J. Biomed. Opt.* **2010**, *15*, 047006.
- (54) Wu, T.C.; Vasudev, M.; Dutta, M.; Stroscio, M.A. Raman and Surface-Enhanced Raman Scattering (SERS) Studies of the Thrombin-Binding Aptamer. *IEEE Trans Nanobioscience* **2013**, *12*, 93-97.
- (55) Barhoumi, A.; Zhang, D.; Halas, N.J. Correlation of Molecular Orientation and Packing Density in a dsDNA Self-Assembled Monolayer Observable with Surface-Enhanced Raman Spectroscopy. *J. Am. Chem. Soc.* **2008**, *130*, 14040-14041.
- (56) Rusciano, G.; De Luca, A.C.; Pesce, G.et al. Label-Free Probing of G-Quadruplex Formation by Surface-Enhanced Raman Scattering. *Anal. Chem.* **2011**, *83*, 6849-6855.
- (57) Marotta, N.E.; Beavers, K.R.; Bottomley, L.A. Limitations of Surface Enhanced Raman Scattering in Sensing DNA Hybridization Demonstrated by Label-Free DNA Oligos as Molecular Rulers of Distance-Dependent Enhancement. *Anal. Chem.* **2013**, *85*, 1440-1446.
- (58) Singh, A.K.; Khan, S.A.; Fan, Z.et al. Development of a Long-Range Surface-Enhanced Raman Spectroscopy Ruler. J. Am. Chem. Soc. **2012**, 134, 8662-8669.
- (59) Myres, G.J.; Harris, J.M. Stable Immobilization of DNA to Silica Surfaces by Sequential Michael Addition Reactions Developed with Insights from Confocal Raman Microscopy. *Anal. Chem.* **2023**, *95*, 3499-3506.
- (60) Myres, G.J.; Peterson, E.M.; Harris, J.M. Confocal Raman Microscopy Enables Label-Free, Quantitative, and Structurally Informative Detection of DNA Hybridization at Porous Silica Surfaces. *Anal. Chem.* **2021**, *93*, 7978-7986.
- (61) Myres, G.J.; Harris, J.M. Nanomolar Binding of an Antibiotic Peptide to DNA Measured with Raman Spectroscopy. *Langmuir* **2023**, *39*, 4150-4160
- (62) Zhao, Y.; Kan, Z.-Y.; Zeng, Z.-X.et al. Determining the Folding and Unfolding Rate Constants of Nucleic Acids by Biosensor. Application to Telomere G-Quadruplex. J. Am. Chem. Soc. 2004, 126, 13255-13264.
- (63) Bhattacharyya, D.; Mirihana Arachchilage, G.; Basu, S. Metal Cations in G-Quadruplex Folding and Stability. *Front. Chem. (Lausanne, Switz.)* **2016**, *4*.

- (64) Russo Krauss, I.; Merlino, A.; Randazzo, A.et al. High-resolution structures of two complexes between thrombin and thrombin-binding aptamer shed light on the role of cations in the aptamer inhibitory activity. *Nucleic Acids Res.* **2012**, *40*, 8119-8128.
- (65) Xiao, Y.; Uzawa, T.; White, R.J.; DeMartini, D.; Plaxco, K.W. On the Signaling of Electrochemical Aptamer-Based Sensors: Collision- and Folding-Based Mechanisms. *Electroanalysis* **2009**, *21*, 1267-1271.
- (66) Kitt, J.P.; Harris, J.M. Confocal Raman Microscopy for in Situ Detection of Solid-Phase Extraction of Pyrene into Single C18–Silica Particles. *Anal. Chem.* **2014**, *86*, 1719-1725.
- (67) Brandt, N.N.; Brovko, O.O.; Chikishev, A.Y.; Paraschuk, O.D. Optimization of the Rolling-Circle Filter for Raman Background Subtraction. *Appl. Spectrosc.* **2006**, *60*, 288-293.
- (68) Burge, S.; Parkinson, G.N.; Hazel, P.; Todd, A.K.; Neidle, S. Quadruplex DNA: sequence, topology and structure. *Nucleic Acids Res.* **2006**, *34*, 5402-5415.
- (69) Huppert, J.L. Four-stranded nucleic acids: structure, function and targeting of G-quadruplexes. *Chem. Soc. Rev.* **2008**, *37*, 1375-1384.
- (70) Padmanabhan, K.; Padmanabhan, K.P.; Ferrara, J.D.; Sadler, J.E.; Tulinsky, A. The structure of alpha-thrombin inhibited by a 15-mer single-stranded DNA aptamer. *J. Biol. Chem.* **1993**, *268*, 17651-17654.
- (71) Friedman, S.J.; Terentis, A.C. Analysis of G-quadruplex conformations using Raman and polarized Raman spectroscopy. *J. Raman Spectrosc.* **2016**, *47*, 259-268.
- (72) Lawton, W.H.; Sylvestre, E.A. Self Modeling Curve Resolution. *Technometrics* **1971**, *13*, 617-633.
- (73) Malinowski, E.R.; Cox, R.A.; Haldna, U.L. Factor analysis for isolation of the Raman spectra of aqueous sulfuric acid components. *Anal. Chem.* **1984**, *56*, 778-781.
- (74) Malinowski, E.R. Factor Analysis in Chemistry (2nd edition); John Wiley and Sons: New York, 1991.
- (75) Kitt, J.P.; Bryce, D.A.; Minteer, S.D.; Harris, J.M. Confocal Raman Microscopy Investigation of Self-Assembly of Hybrid Phospholipid Bilayers within Individual Porous Silica Chromatographic Particles. *Anal. Chem.* **2019**, *91*, 7790-7797.
- (76) Marathias, V.M.; Bolton, P.H. Determinants of DNA Quadruplex Structural Type: Sequence and Potassium Binding. *Biochemistry* **1999**, *38*, 4355-4364.
- (77) Marathias, V.M.; Bolton, P.H. Structures of the potassium-saturated, 2:1, and intermediate, 1:1, forms of a quadruplex DNA. *Nucleic Acids Res.* **2000**, *28*, 1969-1977.

- (78) Rygula, A.; Majzner, K.; Marzec, K.M.*et al.* Raman spectroscopy of proteins: a review. *J. Raman Spectrosc.* **2013**, *44*, 1061-1076.
- (79) Padmanabhan, K.; Tulinsky, A. An Ambiguous Structure of a DNA 15-mer Thrombin Complex. *Acta Crystallogr.*, *Sect. D: Biol. Crystallogr.* **1996**, *52*, 272-282.
- (80) Pagano, B.; Martino, L.; Randazzo, A.; Giancola, C. Stability and Binding Properties of a Modified Thrombin Binding Aptamer. *Biophys. J.* **2008**, *94*, 562-569.
- (81) Baaske, P.; Wienken, C.J.; Reineck, P.; Duhr, S.; Braun, D. Optical Thermophoresis for Quantifying the Buffer Dependence of Aptamer Binding. *Angew. Chem. Int. Ed.* **2010**, *49*, 2238-2241.
- (82) Mears, K.S.; Markus, D.L.; Ogunjimi, O.; Whelan, R.J. Experimental and mathematical evidence that thrombin-binding aptamers form a 1 aptamer:2 protein complex. *Aptamers (Oxf)* **2018**, *2*, 64-73.
- (83) Duguid, J.G.; Bloomfield, V.A.; Benevides, J.M.; Thomas, G.J., Jr. DNA melting investigated by differential scanning calorimetry and Raman spectroscopy. *Biophys. J.* **1996**, *71*, 3350-3360.
- (84) Sancar, A.; Sancar, G.B. DNA Repair Enzymes. Annu. Rev. Biochem 1988, 57, 29-67.
- (85) Fleming, A.M.; Ding, Y.; Burrows, C.J. Oxidative DNA damage is epigenetic by regulating gene transcription via base excision repair. *Proc. Natl. Acad. Sci. U. S. A.* **2017**, *114*, 2604-2609.
- (86) Tate, P.H.; Bird, A.P. Effects of DNA methylation on DNA-binding proteins and gene expression. *Curr. Opin. Genet. Dev.* **1993**, *3*, 226-231.
- (87) Buck-Koehntop, B.A.; Defossez, P.-A. On how mammalian transcription factors recognize methylated DNA. *Epigenetics* **2013**, *8*, 131-137.

# TOC Graphic

